A&A manuscript no.
(will be inserted by hand later)

Your thesaurus codes are:
03 (11.03.1; 11.09.3; 12.03.3; 12.03.4; 12.04.1; 13.25.2)

ASTRONOMY
AND
ASTROPHYSICS

The effect of magnetic fields on the mass determination of clusters of galaxies

K. Dolag[1], **S. Schindler**[2]

[1] MPI für Astrophysik, Karl-Schwarzschild-Str. 1, 85748 Garching, Germany; e-mail: kdolag@mpa-garching.mpg.de
[2] Astrophysics Research Institute, Liverpool John Moores University, Twelve Quays House, Egerton Wharf, Birkenhead CH41 1LD, United Kingdom; e-mail: sas@staru1.livjm.ac.uk

Abstract. We test the effects of magnetic fields on the mass determination of galaxy clusters with the X-ray method. As this method takes into account only thermal pressure, additional non-thermal pressure support, e.g. caused by a magnetic field, can result in an underestimation of the mass. SPH models of galaxy clusters including magnetic fields of various strengths in two different cosmologies are used for the test. We compare the true mass of the model clusters with the mass determined from simulated X-ray images of the same models. The effect of the magnetic field on the mass in relaxed clusters is found to be negligible compared to other uncertainties, even at small radii, where the strongest effects are expected. However in one model, in which the cluster is in the process of merging, we find an effect of up to a factor of 2 caused by the magnetic field. In relaxed clusters the mass estimate, averaged over many models, is at most 15% smaller in models with relatively high magnetic field of 2μG compared to models without a magnetic field with a small dependence on the cosmology chosen. Therefore we conclude that the presence of a magnetic field cannot be responsible for the discrepancies of a factor of 2-3 found between X-ray and lensing mass in the central regions of relaxed clusters.

Key words: Galaxies: clusters: general – intergalactic medium – Cosmology: observations – Cosmology: theory – dark matter – X-rays: galaxies

1. Introduction

Clusters of galaxies – the most massive bound objects in the universe – are excellent diagnostic tools for cosmological parameters. In particular, measuring the masses of clusters provides a way to determine the amount and the distribution of dark matter and thus $\Omega_{\rm m}$. The comparison with the baryonic component yields an estimate for $\Omega_{\rm baryon}$, which is another important cosmological parameter, as current measurements are in contradiction with primordial nucleosynthesis for a $\Omega = 1$ universe (White et al. 1993).

Cluster masses can be measured in various ways, via the gravitational lensing effect, via the assumption of virial equilibrium and with X-ray observations using the assumption of hydrostatic equilibrium. In some clusters these different methods yield masses which can differ up to a factor of three in the central region of the cluster with the lensing mass being typically larger, e.g. A2218 (Kneib et al. 1995; Squires et al. 1996), MS0440+0204 (Gioia et al. 1998), RXJ1347-1145 (Fischer & Tyson, 1997, Schindler et al. 1997; Sahu et al. 1998), Cl0939+4713 (Seitz et al. 1996; Schindler et al. 1998). Various reasons for these discrepancies have been suggested. The presence of substructure and cluster mergers are obvious ways to explain the differences, but tests with numerical simulations showed that the assumptions of hydrostatic equilibrium and spherical symmetry are well justified in relaxed clusters of galaxies (Evrard et al. 1996; Schindler 1996) and cannot account for the large discrepancies in relaxed clusters. Also the effects of small-scale density variations were found to be much smaller than the observed discrepancies (Mathiesen et al. 1999). As a further possibility for the discrepancies, in particular in the cluster centres, Loeb & Mao (1994) suggested that the intra-cluster gas might not only be supported by thermal pressure, but also by considerable magnetic pressure. As magnetic pressure is not taken into account in the X-ray mass determination method it potentially leads to an underestimation of the mass.

Whereas Loeb & Mao (1994) suggested that strong magnetic fields can be hidden to Faraday rotation measurements if the magnetic fields are tangled, Dolag et al. (1999) found in simulations that even clusters with an overall small magnetic field can be penetrated partially by regions of high magnetic fields. These simulations are based on a consistent model for the cluster magnetic field and therefore lead to realistic magnetic field configurations within the assumed cosmological scenarios. Here the magnetic fields strengths and structure is given by the formation of the cluster in a cosmological environment. Although on average the magnetic pressure in there models is much smaller than the thermal pressure ($\approx$ 5% (Dolag et al. 2000b)), the models show some scatter around this mean value. There are domains of high magnetic fields approaching

model	H_0	Ω_0	Λ	σ_8	z_0	$f_{\rm baryon}$
EdS	0.5	1.0	0.0	1.2	15	5%
FlatLow	0.7	0.3	0.7	1.05	20	10%

Table 1. Parameters of the EdS and the FlatLow models.

model	$B_{\rm ini}$	$\langle B_{\rm final}\rangle^{\rm EdS}_{\rm core}$	$\langle B_{\rm final}\rangle^{\rm FlatLow}_{\rm core}$
no B	$0.0\,{\rm G}$	—	—
low B	$0.2\times10^{-9}\,{\rm G}$	$0.4\,\mu{\rm G}$	$0.3\,\mu{\rm G}$
medium B	$1.0\times10^{-9}\,{\rm G}$	$1.1\,\mu{\rm G}$	$0.8\,\mu{\rm G}$
high B	$5.0\times10^{-9}\,{\rm G}$	$2.5\,\mu{\rm G}$	$2.0\,\mu{\rm G}$

Table 2. Initial magnetic fields (column 2) and the resulting final magnetic field strengths in the clusters (column 3 and 4 for EdS and FlatLow models, respectively). The final values are an average of the magnetic field over the central region (within a radius of 350 kpc) of all ten clusters for each cosmology.

or sometimes even exceeding equipartition with the thermal energy. The simulations predict the number, locations and sizes of these domains depending on the formation history and dynamical state of the cluster, which provides the possibility to test the importance of these domains. So far the influence of these domains on the mass determination is not clear.

In this work we use the models by Dolag et al. (1999) to test the influence of such magnetic fields on the mass determination with the X-ray method. We compare the true cluster mass, which is known exactly for the model clusters, with the mass derived from a simulated X-ray observation of the same model cluster.

After the description of the method in Sect. 2 we present the results in Sect. 3 and the conclusions in Sect. 4.

2. Method

We use the cosmological MHD code described in Dolag et al. (1999) to simulate the formation of magnetised galaxy clusters from an initial density perturbation field. The code combines the merely gravitational interaction of a dark-matter component with the hydrodynamics of a gaseous component. The gravitational interaction of the particles is evaluated on GRAPE boards (Sugimoto et al. 1990), while the gas dynamics is computed in the SPH approximation (Lucy 1977, Gingold & Monaghan 1977). It is supplemented with the magneto-hydrodynamic equations to trace the evolution of magnetic fields which are frozen into the motion of the gas due to its assumed ideal electric conductivity. The back-reaction of the magnetic field onto the gas is included. The code assumes the intra-cluster medium to be an ideal gas with adiabatic index of $\gamma = 5/3$. Radiative cooling is not included. As the surroundings of clusters are important because their tidal fields affect the overall cluster structure and the merging history, the simulation volumes are surrounded by a layer of boundary particles whose purpose it is to represent accurately the tidal fields in the cluster neighbourhood. Extensive tests of the code were performed and described in Dolag et al. (1999). Various test problems could be solved successfully, and $\nabla\cdot\mathbf{B}$ is always negligible compared to the magnetic field divided by a typical length scale.

Two different kinds of cosmological models are used, EdS and FlatLow (see Table 1). We set up cosmological initial conditions at redshift $z = 15$ (for EdS) and $z = 20$ (for FlatLow) and follow the formation of the clusters including the magnetic field. For each cosmology we calculate ten different realisations which result in clusters of different final masses and different dynamical states at redshift $z = 0$.

We simulate each of these clusters with different initial magnetic fields, listed in Table 2, yielding a total of 80 cluster models. Since the origin of magnetic fields on cluster scales is unknown, we use either completely homogeneous or chaotic initial magnetic field structures. The evolution of the intracluster fields is then computed during cluster collapse. Previous work showed that (i) the initial field structure is irrelevant because the final field structure is determined by the dynamics of the cluster collapse, and (ii) the initial field strengths of *medium B* at the starting redshift (see Table 1) are adequate to reproduce the Faraday-rotation statistics by Kim et al. (1991). The simulated and the observed rotation-measure distributions could not be distinguished significantly by a Kolmogorov-Smirnov test. However, the scatter is large because of the relatively small number of simulated clusters per set (only 10 cluster for each cosmology) and because of selection effects both in the simulations and the observations. We therefore allow for a range of initial magnetic field strengths resulting in a range of synthetic Faraday-rotation distributions which are all well in agreement with the observed data. The steep power spectrum of these magnetic fields suggests that the contribution to the energy density by fields tangled on scales smaller than the resolution of the simulation ($\gtrsim$ 30kpc) is negligible. A detailed description of these models and a comparison with rotation measures is given in Dolag et al. (1999). With a realistic model for distributing relativistic electrons in the simulated clusters, the simulations are also able to match the properties of observed radio halos very well (see Dolag & Ensslin 2000). As both initial conditions are equivalent for the final clusters we choose the homogeneous initial field set-up, because it is numerically easier to handle.

Due to compression and turbulence in the gas flow, the magnetic field is highest in and near the centres of the simulated clusters. Here the thermal pressure has also the highest values, which leads to almost constant ratio of magnetic to thermal pressure support across a large range of cluster-centric radii, which can amount to $\approx 5\%$ for EdS cosmologies and slightly lower values in the FlatLow cosmologies (Dolag et al. 2000b). The overall structure of the magnetic field in the outer regions of the clusters differs from that near the cluster centre. Accretion and merger events arrange the magnetic fields in the outer cluster regions in coherent patterns on fairly large scales. Near the cluster centre, the gas flow pattern is almost randomised, and the magnetic field is consequently tangled and bent on fairly small scales ($\approx$ 70kpc). Although the magnetic pressure can be considered isotropic at or near the cluster cen-

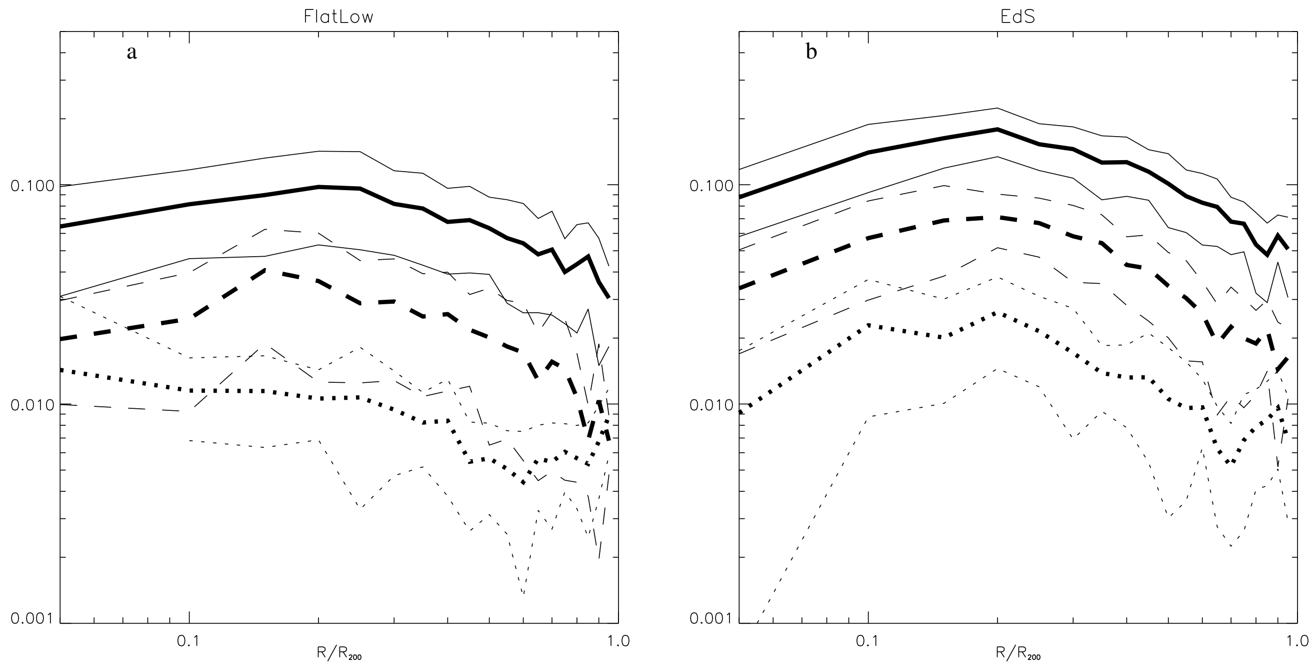

Fig. 1. Percentage of particles for which the ratio between magnetic and thermal pressure exceeds of 5% as function of position in the cluster (thick lines). Shown is the average over all FlatLow models (a) and all EdS models (b). The different line types distinguish the different magnetic fields, with the solid line representing a high, the dashed line a medium and the dotted line a low magnetic field. The thin lines are the RMSs between the models of the same class. The radial distance to the cluster centre is in units of the virial radius R_{200}.

tre, it may well be anisotropic in the outer parts. Even though the fraction of the magnetic pressure relative to the thermal pressure, averaged over spherical shells, is approximately constant across the cluster, the detailed effects of magnetic pressure on the gas flow depend on the direction of the magnetic field relative to other locally preferred directions, like e.g. the orientation of filaments surrounding a cluster, the local path of matter infall, or the orbit of a merging sub-clump. Therefore, the same overall magnetic pressure can have different effects on the local dynamics of gas flows, depending on whether the magnetic field is ordered on scales comparable to the cluster scale, and on the orientation of the magnetic field. Furthermore in an intra-cluster medium with a small averaged fraction of the magnetic relative to the thermal pressure may be well regions, in which the magnetic field gives much stronger pressure support. Fig. 1 shows the mass fraction inside spherical shells which have more than 5% magnetic pressure support. Note that there is even a small number of regions where the magnetic pressure is twice as high as the thermal pressure.

In this work we concentrate on the effects of the magnetic field on the mass determination via the X-ray method. Effects like deviation from hydrostatic equilibrium due to mergers, possible shortcomings of the β model and others are not discussed. In order not to mix up the different effects we select for the mass tests only the models not suffering from the above mentioned other effects, i.e. relaxed clusters. Otherwise even the average over many models can be dominated by the strong deviations of a single model. Furthermore, a small magnetic field can slightly alter the dynamical time scale of a simulated cluster. Therefore, when comparing simulated clusters with different magnetic fields at equal redshifts, they can be in slightly different evolutionary stages according to their own time scale. While this effect is irrelevant in relaxed clusters it can change the mass estimate considerably for merging clusters.

cosmology	FlatLow	EdS
used clusters	6/10	7/10
no B	0.98 ± 0.31	0.85 ± 0.32
low B	1.08 ± 0.25	0.81 ± 0.28
medium B	0.98 ± 0.26	0.96 ± 0.43
high B	1.02 ± 0.22	0.77 ± 0.32

Table 3. Ratio of true mass to X-ray mass at $50\mathrm{kpc}$ for 4 different magnetic field strengths in both cosmologies: Mean value and standard deviation of 21 and 18 model configuration for EdS and FlatLow, respectively. For each model we use 3 projections.

To minimize all non-magnetic effects we select 6 out of the FlatLow models and 7 out of the EdS models, which look round and relaxed and are not in the process of merging at the moment of the mass determination ($z = 0$).

To calculate X-ray masses from these model clusters, we project the model clusters onto X-ray images in three projection directions. We use the ROSAT energy range (0.1-2.4 keV) for these projections, because for typical cluster temperatures the observed countrate in this range is almost independent of the temperature. We calculate maps of projected emission-weighted temperature as well. Both projections are binned to 200×200 pixels with a resolution of 20 kpc. The bin size determines the smallest possible radius for our mass analysis. We can measure masses only at radii larger than about 2 pixels, i.e. $\approx$ 50 kpc. From X-ray and temperature maps we calculate surface brightness and temperature profiles centred on the X-ray centroid. We deproject the surface brightness to three-dimensional densities with the β model (Cavaliere & Fusco-Femiano 1976). With the assumption of hydrostatic equilibrium the integral mass within radius r can be determined as

$$M(r) = \frac{-kr}{\mu m_p G} T \left(\frac{d \ln \rho}{d \ln r} + \frac{d \ln T}{d \ln r} \right), \qquad (1)$$

with ρ and T being the density and the temperature of the intracluster gas, respectively. k, μ, m_p, and G are the Boltzmann constant, the molecular weight, the proton mass, and the gravitational constant.

3. Results

For the comparison of the true masses of the models and the masses derived by the X-ray method we calculate the ratio of both and plot this ratio versus radius. Figure 2a and b show the comparison for FlatLow and EdS models, respectively. The ratio profiles are averaged over various models and three projection directions (but not over different initial magnetic fields).

There is an overall underestimation of the mass visible at very large and very small radii, which is not due to the magnetic field, but to limitations of the β model. As shown in Fig. 3 the β model cannot fit every part of the profile equally well. Typically, the β model is less steep than the actual profile in the central region and at large radii. Therefore the density gradients are underestimated there, which leads to an underestimation of the mass in these regions according to Eq. (1). A detailed investigation of different analytic deprojection methods will be published in a forthcoming paper.

As expected the effects of the magnetic field are largest in the central regions because the magnetic field is generally stronger in the cluster centre as seen in simulations (Dolag et. al 1999) as well as in observations (Kim et al. 1990; Clark et al. 1999). Mostly profiles for high magnetic fields are slightly below the profiles for no or low magnetic field. The values of the mass ratios at 50 kpc are listed in Table 3. The difference between the profiles at this radius is only 10-15%. For comparison the standard deviations of the profiles are shown as well. Clearly, the differences between the profiles with different magnetic field are much smaller than the scatter due to other effects like projection effects. Therefore they are certainly not significant. Moreover, the curves are not even exactly ordered according to the magnetic field strength. At radii larger than 200 kpc there is no difference at all between the profiles of models with different magnetic fields. This comparison of the profiles shows that the mass differences for different magnetic fields are negligible at all radii.

One of the merger models, which is not used for the profiles in Fig. 2, shows an interesting effect. The mass ratios are clearly ordered according to the magnetic field (see Fig. 4). As

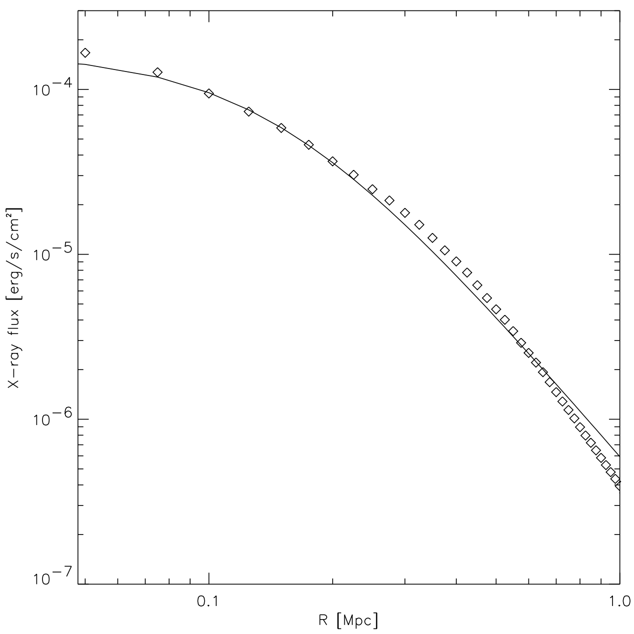

Fig. 3. X-ray surface brightness profile (diamonds) for one of the relaxed clusters from the EdS models. The solid line shows the fit of these data with a β-model. Obviously, the β model is too flat in the central region as well as at large radii. Therefore the gradients are underestimated by the β model in these regions, which results in an underestimation of the mass according to Eq. 1.

it is a merger of two nearly equal subclusters, the mass estimate is very sensitive on the exact density distribution in the central region and the positions of the shocks and therefore mass over- or underestimations are expected. But if these were the only effects one would not expect the profiles to be ordered according to the magnetic field as seen in Fig. 4. Obviously, the magnetic field can be important in such extreme merger cases. This is plausible because magnetic fields are enhanced during collisions of clusters.

4. Discussion and Conclusions

A magnetic field can affect the mass determination in a cluster of galaxies in principle in two ways, by the isotropic and the anisotropic component of the magnetic pressure. The isotropic component provides an additional non-thermal pressure support, hence tends to lower the temperature in the cores of clusters. Depending on the gas mass fraction, this effect can amount to $\approx$ 5% of the central temperatures for EdS cosmologies (Dolag et al. 2000). Consequently, the mass is underestimated by the X-ray method because this additional pressure is not taken into account. The anisotropic component of the magnetic pressure slightly changes the density and temperature distribution in the inner region of the cluster by redirecting gas flows. In this way the gas is prevented from reaching hydrostatic equilibrium. This may also lead to a possible misinterpretation of the X-ray emission when determining the mass.

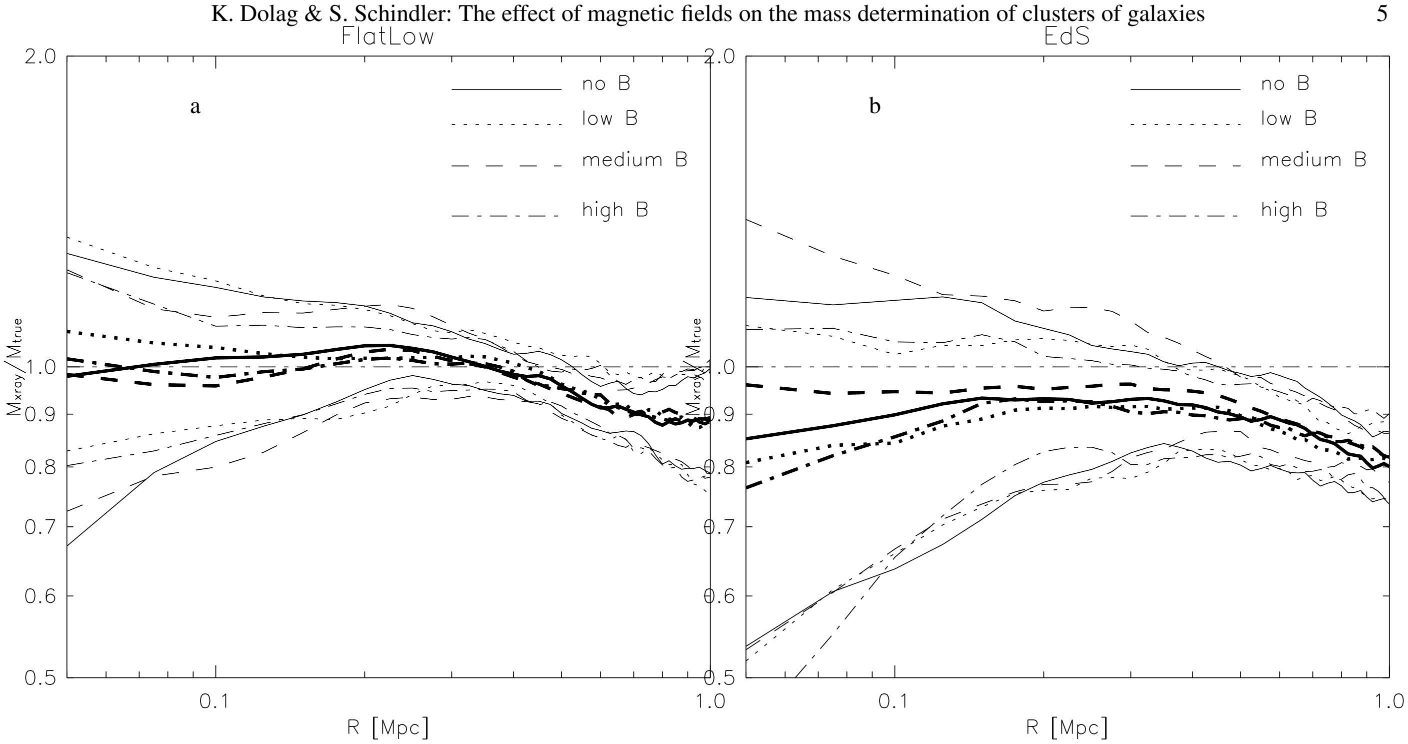

Fig. 2. Ratio of true and X-ray mass for 4 different magnetic field strengths in two different cosmologies. The bold lines are averaged profiles, while the thin lines show the corresponding standard deviation. a) The FlatLow model profiles are averaged over 18 configurations (6 models × 3 projections). b) The EdS model profiles are averaged over 21 configurations (7 models × 3 projections). In general there are only a marginal trends to underestimate the mass with increasing magnetic field strength. This effect is much smaller than the standard deviation and therefore not significant.

To test these effects, we performed cosmological MHD simulations of galaxy clusters in different cosmologies, to examine the effect of magnetic fields in galaxy clusters on the mass reconstruction via the X-ray method. The range of initial magnetic field strengths was chosen so as to reproduce the observed Faraday-rotation measurements at the final redshift of $z = 0$.

We find one extreme merger model, in which the sum of all effects caused by the magnetic field can reduce the reconstructed mass by a factor of 2 in the central region. This model cluster is in the process of merging and has therefore a particularly high magnetic field. As the mass determination for merging clusters canbe unreliable, because they are far from hydrostatic equilibrium, this adds up to already large uncertainties, so that we can just emphasise again, that X-ray mass estimates of merging clusters must be regarded with caution.

In relaxed clusters magnetic fields do not generally lead to any under- or overestimate of masses and they cannot be the dominant reason for the mass discrepancy between X-ray mass and lensing mass found in the central region of some clusters. The maximum difference of averaged mass profiles between models with high magnetic field and no magnetic field is 15%, while observational discrepancies between different methods of a factor of 2-3 are found. It is more likely that projection effects play an important role. As the gravitational lensing effect is sensitive to all the mass along the line-of-sight while the X-ray mass determines only the mass in the potential well, other mass concentrations along the line-of-sight can lead to a higher lensing mass compared to the X-ray mass (as probably seen in Cl0500-24 (Schindler & Wambsganss 1997)). Another effect can be that cooling flows lead to wrong determinations of temperatures when the temperature profile of the cluster is not available (Allen 1998). Also the β model does not always provide a good fit to the profile at all radii (Bartelmann & Steinmetz 1996). All these effects will be analysed in detail in a forthcoming paper.

Acknowledgements. We thank Phil James for carefully reading the manuscript.

References

Allen S.W, 1998, MNRAS 296, 392
Bartelmann, M., Steinmetz, M., 1996, MNRAS, 283, 431
Cavaliere A., Fusco-Femiano R., 1976, A&A 49, 137
Clarke T.E., Kronberg P.P., Böhringer H., 1999, in: Diffuse thermal and relativistic plasma in galaxy clusters, Böhringer H., Feretti L., Schuecker P. (eds.), MPE report 271, 82
Dolag K., Bartelmann M., Lesch H., 1999, A&A 348, 351
Dolag, K., Ensslin, T., 2000, accepted for publication in A&A
Dolag K., Evrard A., Bartelmann M., 2000, submitted to A&A
Fischer P., Tyson J.A., 1997, AJ 114, 14
Gingold, R. A., Monaghan, J. J., 1977, MNRAS 181, 375
Gioia I.M., Shaya E.J., Le Fèvre O., et al., 1998, ApJ 497, 573
Kim K.T., Kronberg P.P., Dewdney P.E., Landecker T.L., 1990, ApJ 355, 29
Kim K.T., Kronberg P.P., Tribble P.C., 1991, ApJ, 379, 80

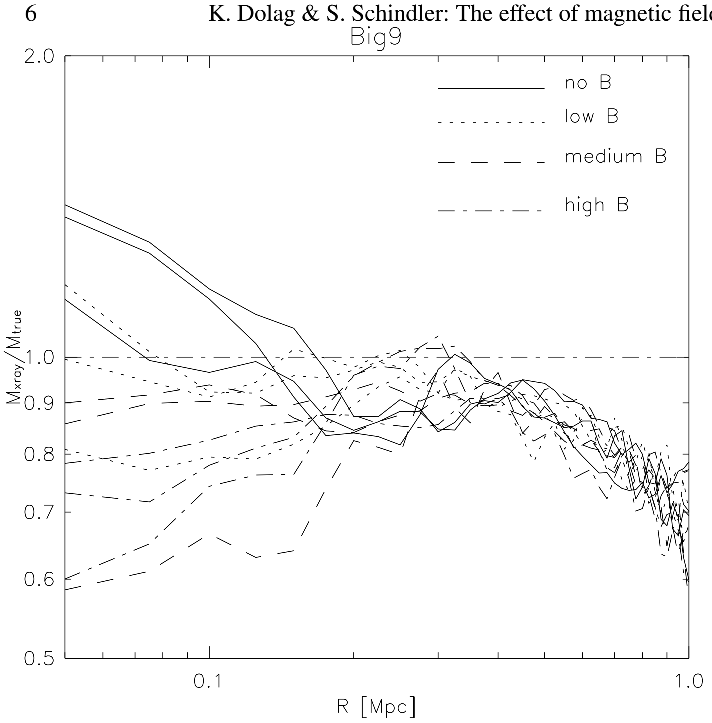

Fig. 4. Ratio of true and X-ray mass for one of the EdS models, in which the subclusters are in the process of merging. For each model, the three projection directions are shown in the same line style. The ordering from over- to underestimating the mass according to the magnetic field strengths (different line styles) is a result of the combination of all effects due to the magnetic field mentioned in the text. For this extreme merger the magnetic effects are considerably larger than the usual scatter of mass profiles from different projection directions.

Kneib J.-P., Mellier Y., Pello R., et al., 1995, A&A 303, 27
Loeb A., Mao S., 1994, ApJ 435, L109
Lucy L., 1977, AJ 82, 1013
Mathiesen B., Evrard A.E., Mohr J.J., 1999, ApJ 520, L21
Evrard A.E., Metzler C.A., Navarro J., 1996, 469, 494
Sahu K., Shaw R.A., Kaiser M.E., et al., 1998, ApJ 492, L125
Schindler S., 1996, A&A 305, 756
Schindler S., Wambsganss J., 1997, A&A 322, 66
Schindler S., Hattori M., Neumann D.M., Böhringer H., 1997, A&A 317, 646
Schindler S., Belloni P., Ikebe Y., et al., 1998, A&A 338, 843
Seitz C., Kneib J.-P., Schneider P., Seitz S., 1996, A&A 314, 707
Squires G., Kaiser N., Babul A., et al., 1996, ApJ 461, 572
Sugimoto D., Chikada Y., Makino J., et al., 1990, Nat. 345, 33
White S.D.M., Navarro J.F., Evrard A.E., Frenk C.S., 1993, Nat. 366, 429